



Published in final edited form as:

Proteins. 2009 February 1; 74(2): 526–529. doi:10.1002/prot.22278.

Crystal structure of human retinoblastoma binding protein 9 (RBBP9)

Sergey M. Vorobiev¹, Min Su¹, Jayaraman Seetharaman¹, Yuanpeng Janet Huang², Chen X. Chen², Melissa Maglaqui², Haleema Janjua², Michael Proudfoot³, Alexander Yakunin³, Rong Xiao², Thomas B. Acton², Gaetano T. Montelione², and Liang Tong^{1,*}

¹Department of Biological Sciences, Northeast Structural Genomics Consortium, Columbia University, New York, NY 10027

²Center for Advanced Biotechnology and Medicine, Department of Molecular Biology and Biochemistry, Rutgers University, Department of Biochemistry, Robert Wood Johnson Medical School, Northeast Structural Genomics Consortium, Piscataway, NJ 08854

³Structural Proteomics in Toronto, Banting and Best Department of Medical Research University of Toronto, Toronto, Ontario M5G 1L6, Canada

As a step towards better integrating protein three-dimensional (3D) structural information in cancer systems biology, the Northeast Structural Genomics Consortium (NESG) (www.nesg.org) has constructed the Human Cancer Pathway Protein Interaction Network (HCPIN) by analysis of several classical cancer-associated signaling pathways and their physical protein-protein interactions 1. Many well-known cancer-associated proteins play central roles as "hubs" or "bottlenecks" in the HCPIN (<http://nmr.cabm.rutgers.edu/hcpin>). NESG has selected more than 1,000 human proteins and protein domains from the HCPIN for sample production and 3D structure determination 1. The long-range goal of this effort is to provide a comprehensive 3D structure-function database for human cancer-associated proteins and protein complexes, in the context of their interaction networks.

Human retinoblastoma binding protein 9 (RBBP9) is one of the HCPIN proteins targeted by NESG. RBBP9 was initially identified as the product of a new gene, Bog (for B5T over-expressed gene), in several transformed rat liver epithelial cell lines resistant to the growth-inhibitory effect of TGF- β 1 as well as in primary human liver tumours 2,3. RBBP9 contains the retinoblastoma (Rb) binding motif LxCxE in its sequence, and was shown to interact with Rb by yeast two-hybrid and co-immunoprecipitation experiments 2. Mutation of the Leu residue in this motif to Gln blocked the binding to Rb. RBBP9 can displace E2F1 from E2F1-Rb complexes, and over-expression of RBBP9 overcomes TGF- β 1 induced growth arrest and results in transformation of rat liver epithelial cells leading to hepatoblastoma-like tumours in nude mice 2. RBBP9 may also play a role in cellular responses to chronic low dose radiation 4. A close homolog of RBBP9, sharing 93% amino acid sequence identity and also known as RBBP10 5, interacts with a protein with sua5-yciO-yrdC domains 6.

Amino acid sequence analysis suggests that RBBP9 belongs to the DUF1234 superfamily and may have the α/β hydrolase fold. The closest sequence homolog with structural information is that of the YdeN protein from *Bacillus subtilis* 7, which shares only 26% sequence identity with RBBP9 (Fig. 1). We report here the crystal structure of the 21 kD human RBBP9 at 1.72 Å resolution.

*Corresponding author. Phone: (212) 854-5203; FAX: (212) 865-8246, e-mail: ltong@columbia.edu.

The crystal structure of human RBBP9 has been determined at 1.72 Å resolution by the seleno-methionyl single-wavelength anomalous diffraction method 8. The final refined atomic model contains residues 3-186 and 3-182 of the two RBBP9 molecules in the crystallographic asymmetric unit, with excellent agreement with the crystallographic data and ideal geometric parameters (Table 1). RBBP9 behaves as a monomer in solution based on analytical gel filtration and static light scattering experiments (data not shown), and the two molecules in the asymmetric unit do not show strong interactions between them. The atomic coordinates and structure factors have been deposited in the Protein Data Bank, with the accession code 2QS9.

The structure of RBBP9 has the α/β hydrolase fold, consisting of a central sixstranded parallel β -sheet with topology order 213456 surrounded by seven α -helices (Fig. 2A). The putative active site of this hydrolase is located at the top of the β -sheet, with the triad Ser75-His165-Asp138. As in other α/β hydrolases, Ser75 is located in a nucleophile elbow 9, a tight turn connecting strand β 3 and helix α C, and assumes a strained main-chain conformation. The side chains of these three residues are hydrogenbonded to each other in the structure and Ser75 is located in a prominent groove on the surface of the protein (Fig. 2B), suggesting that RBBP9 could have hydrolase activity. However, the natural substrate of this putative enzyme is currently not known. Members of the DUF1234 superfamily include acyl transferases, chlorophyllase (chlase), lipase, thioesterase, serine carboxypeptidase and others.

In an attempt to obtain experimental evidence for catalytic activity of RBBP9, the purified protein was subjected to an array of general enzymatic assays 10. They included assays for phosphatase (with *p*-nitrophenyl phosphate as substrate), phosphodiesterase (with bis-*p*-nitrophenyl phosphate), dehydrogenase or oxidase (with several pools of substrates: amino acids, carbohydrates, alcohols, and aldehydes), protease (with several chromogenic substrates: BAPNA, Pro-pNA, Suc-AAA-pNA, and Suc-Phe-pNA), carboxylesterase (with *p*-NP-palmitate), and thioesterase (with palmitoyl-CoA). The results show that RBBP9 does not possess enzymatic activity towards any of the substrates under the conditions tested. It remains possible, however, that RBBP9 has activity towards other substrates.

The protein with the highest structural similarity to RBBP9 is the homologous YdeN gene product from *Bacillus subtilis* 7, with 26% sequence identity. The rms distance between equivalent C α atoms of the two structures is 1.7 Å. The putative catalytic triad of YdeN, Ser71-His164-Asp137, is located in the same position as in RBBP9, although an enzymatic activity has not been demonstrated for this protein either 7. Structural similarity is also observed with a large number of other α/β hydrolases, with rms distance of about 2.5 Å. The sequence identity with these other enzymes is only in the 10–20% range.

In contrast to the putative catalytic site, the LxCxE motif that is important for Rb binding is not present in YdeN and other α/β hydrolases. The Leu residue is located at the end of helix α B, and the other residues are in the loop connecting helix α B and strand β 3, near the bottom of the central β -sheet and far from the putative active site of RBBP9 (Fig. 2A). Somewhat surprisingly, the side chains of both the Leu and the Cys residues are buried in the hydrophobic core of the structure and essentially not accessible to solvent. Only the side chain of the Glu residue is exposed. A conformational change is needed for this motif to directly mediate interactions with Rb. Alternatively, this binding may involve a different surface area of RBBP9, and the LxCxE motif plays an indirect role.

Materials and Methods

Expression and purification of human RBBP9 (Northeast Structural Genomics Consortium (NESG) target HR2978) was carried out as a part of the established high throughput protein production pipeline 11. Briefly, the RBBP9 gene was isolated by RTPCR from human poly-A RNA (Clontech) and cloned into a pET21 derivative (Novagen) yielding plasmid HR2978-21.2 (sequence verified), resulting in a full-length protein with a C-terminal hexahistidine sequence (LEHHHHHH). The selenomethionyl protein was expressed in *Escherichia coli* BL21(DE3)pMgK (a codon supplemented strain), purified using an AKTExpress (GE Healthcare) based two-step protocol consisting of IMAC (HisTrap HP) and gel filtration (HiLoad 26/60 Superdex 75) chromatography. The final yield of purified human RBBP9 (>98% purity by SDS-PAGE; 22.03 kDa by MALDI-TOF mass spectrometry) was about 26 mg/L. The final sample of human RBBP9 was prepared at a concentration of 8.1 mg/ml in a buffer containing 10 mM Tris (pH 7.5), 100 mM NaCl, and 5 mM DTT, flash frozen and stored at -80°C .

The oligomerization state of this sample was analysed as monomer by SEC-MALS measurements performed on an Agilent 1100 HPLC system (Agilent) connected to a triangle light scattering detector and a differential refractometer (miniDAWN Tristar and Optilab, respectively; Wyatt Technology). A Shodex KW-802.5 column (Shodex) was equilibrated in 100 mM Tris-HCl, pH 7.5, 100 mM NaCl, 0.2% NaN_3 at a flow rate of 0.5 ml/min. A sample of RBBP9 in the volume of 30 μl was injected at a concentration of 8.1 mg/ml. Data were processed using ASTRA software (Wyatt Technology) assuming a specific refractive index increment (dn/dc) of 0.185 ml/g. To determine the detector delay volumes and the normalization coefficients for the MALS detector, a BSA sample (Sigma) was used as a reference.

Crystallization screening was performed using a microbatch-under-oil crystallization method at 18°C . After optimization, RBBP9 crystals useful for structure determination were grown in drops composed of 0.5 μL of protein and 0.5 μL of precipitant solution (100 mM Na-acetate (pH 5.0), 100 mM magnesium nitrate, 40% (w/v) PEG4000) under paraffin oil (Hampton Research). The crystals were transferred to paratone oil to remove excess mother liquor before being frozen in liquid propane for data collection at 100K.

A selenomethionyl SAD data set was collected at beamline X4A at the National Synchrotron Light Source. The diffraction data were processed with the HKL2000 package 13. The crystal belongs to space group $P2_1$, with cell parameters of $a=37.1\text{ \AA}$, $b=130.3\text{ \AA}$, $c=39.0\text{ \AA}$, and $\beta=115.9^{\circ}$. There are two molecules of RBBP9 in the crystallographic asymmetric unit.

The programs SHELXE/D 14 and SOLVE 15 were used to locate 6 selenium sites and to calculate phases to 1.8 \AA resolution. Solvent-flattening calculations and partial model building were performed using RESOLVE 15. The model was completed manually using Coot 16 and was refined against 1.72 \AA data with the program CNS 17. Refinement statistics are presented in Table 1. The quality of the model was inspected by the program PROCHECK 18. Figure 2 was created using the program PyMOL 19.

Acknowledgments

We thank Randy Abramowitz and John Schwanof for access to the X4A beamline at NSLS; G. DeTitta of Hauptman Woodward Research Institute for crystallization screening. This research was supported by a grant from the Protein Structure Initiative of the National Institutes of Health (U54 GM074958) and in part by Genome Canada through the Ontario Genomics Institute.

References

1. Huang YJ, Hang D, Lu LJ, Tong L, Gerstein MB, Montelione GT. Targeting the human cancer pathway protein interaction network by structural genomics. *Mol Cell Proteomics*. 2008
2. Voitach JT, Zhang M, Niu C-H, Thorgeirsson SS. A retinoblastoma-binding protein that affects cell-cycle control and confers transforming ability. *Nat Genetics*. 1998; 19:371–374. [PubMed: 9697699]
3. Morris EJ, Dyson NJ. Retinoblastoma protein partners. *Adv Cancer Res*. 2001; 82:1–54. [PubMed: 11447760]
4. Cassie S, Koturbash I, Hudson D, Baker M, Ilnytskyy Y, Rodriguez-Juarez R, Weber E, Kovalchuk O. Novel retinoblastoma binding protein RBBP9 modulates sex-specific radiation responses in vivo. *Carcinogenesis*. 2006; 27:465–474. [PubMed: 16272168]
5. Chen J-Z, Yang Q-S, Wang S, Meng X-F, Ying K, Xie Y, Mao Y-M. Cloning and expression of a novel retinoblastoma binding protein cDNA, RBBP10. *Biochem Genetics*. 2002; 40:273–282. [PubMed: 12296629]
6. Chen J-Z, Ji C, Gu S, Zhao E, Dai J, Huang L, Qian J, Ying K, Xie Y, Mao Y-M. Isolation and identification of a novel cDNA that encodes human yrdC protein. *J Hum Genet*. 2003; 48:164–169. [PubMed: 12730717]
7. Janda I, Devedjiev Y, Cooper D, Chruszcz M, Derewenda U, Gabrys A, Minor W, Joachimiak A, Derewenda ZS. Harvesting the high-hanging fruit: the structure of the YdeN gene product from *Bacillus subtilis* at 1.8 Å resolution. *Acta Cryst*. 2004; D60:1101–1107.
8. Hendrickson WA. Determination of macromolecular structures from anomalous diffraction of synchrotron radiation. *Science*. 1991; 254:51–58. [PubMed: 1925561]
9. Ollis DL, Cheah E, Cygler M, Dijkstra B, Frolova F, Franken SM, Harel M, Remington SJ, Silman I, Schrag J, Sussman JL, Verschuere KHG, Goldman A. The a/b hydrolase fold. *Prot Eng*. 1992; 5:197–211.
10. Proudfoot, M.; Kuznetsova, E.; Sanders, S.; Gonzalez, CF.; Brown, G.; Edwards, AM.; Arrowsmith, CH.; Yakunin, AF. High-throughput screening of purified proteins for enzymatic activity. In: Kobe, B.; Guss, M.; Huber, T., editors. *Methods in Mol Biol. Volume 426, Structural Proteomics: High-throughput methods*. Totowa, NJ: Humana Press; 2008. p. 331–331.
11. Acton TB, Gunsalus K, Xiao R, Ma L, Aramini J, Baron MC, Chiang Y, Clement T, Cooper B, Denissova N, Douglas S, Everett JK, Palacios D, Paranjali RH, Shastry R, Wu M, Ho C-H, Shih L, Swapna GVT, Wilson M, Gerstein M, Inouye M, Hunt JF, Montelione GT. Robotic cloning and protein production platform of the Northeast Structural Genomics Consortium. *Methods Enzymol*. 2005; 394:210–243. [PubMed: 15808222]
12. Chayen NE, Stewart PDS, Maeder DL, Blow DM. An automated system for micro-batch protein crystallization and screening. *J Appl Cryst*. 1990; 23:297–302.
13. Otwinowski Z, Minor W. Processing of X-ray diffraction data collected in oscillation mode. *Method Enzymol*. 1997; 276:307–326.
14. Schneider TR, Sheldrick GM. Substructure solution with SHELXD. *Acta Cryst*. 2002; D58:1772–1779.
15. Terwilliger TC. SOLVE and RESOLVE: Automated structure solution and density modification. *Meth Enzymol*. 2003; 374:22–37. [PubMed: 14696367]
16. Emsley P, Cowtan KD. Coot: model-building tools for molecular graphics. *Acta Cryst*. 2004; D60:2126–2132.
17. Brunger AT, Adams PD, Clore GM, DeLano WL, Gros P, Grosse-Kunstleve RW, Jiang J-S, Kuszewski J, Nilges M, Pannu NS, Read RJ, Rice LM, Simonson T, Warren GL. Crystallography & NMR System: A new software suite for macromolecular structure determination. *Acta Cryst*. 1998; D54:905–921.
18. Laskowski RA, MacArthur MW, Moss DS, Thornton JM. Procheck - a program to check the stereochemical quality of protein structures. *J Appl Cryst*. 1993; 26:283–291.
19. DeLano, WL. *The Pymol manual*. San Carlos, CA: DeLano Scientific;

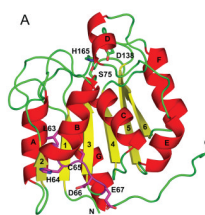


Figure 1.

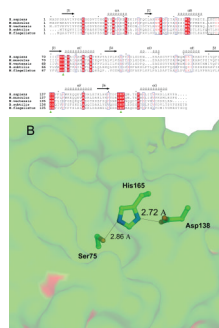


Figure 2.

Table 1

Summary of crystallographic information

Data Collection	
Wavelength (Å)	0.97913
Resolution (Å)	50-1.72
No. of unique reflections	67,796
Redundancy ^a	3.6 (2.8)
Completeness	97 (86)
I/σ(I)	25.9 (14.4)
R _{merge} (%)	4.6 (8.2)
Refinement	
Resolution (Å)	50-1.72
No. of reflections	67,213
No. of protein atoms	2963
No. of water molecules	414
R _{work} (%)	18.3
R _{free} (%) ^b	20.3
rms deviation in bond lengths (Å)	0.005
rms deviation in bond angles (°)	1.3
Average B factor (Å ²)	12.9
<i>Ramachandran plot</i>	
Most favored regions (%)	86.0
Additional allowed regions (%)	14.0
Generously allowed regions (%)	0.0
Disallowed regions (%)	0.0

^aThe numbers in parenthesis are for the high resolution shell (1.78-1.72Å).

^bR_{free} is calculated for 5.0% of randomly selected reflections excluded from refinement.